VII. Summary

As seen from the above discussion there are a wide variety of military applications for fiber optics and integrated optics technology. The fiber optics application are certainly furthest along in terms of practical development. However, future generations of applications will almost certainly have integrated optical circuits. Only then will the full potential advantages of this technology be realized.

This technological area is not without problems. There are serious materials fabrication problems. Radiation sensitivity of these optical materials is a potentially serious problem area that has not been discussed.

It is probably fair to conclude that the military-related applications of this technology are nearer term than those of the telecommunication industry. Further, the impetus provided by military needs will lead to successful applications of fiber optics and integrated optics in the near future.

References

[1] R. A. Andrews, "Optical waveguides and integrated optics technology," NRL Rep. 7291, Aug. 1971.

[2] A. F. Milton and L. W. Brown, "Nonreciprocal access to multiterminal optical data highways," in *Dig. Tech. Papers IEEE/OSA Conf. Laser Engineering and Applications* (Washington, D. C.), May 30, 1973, pp. 24–25.

[3] J. E. Keifer, J. A. Nussmeier, and F. E. Goodwin, "Intracavity CdTe modulators for CO_2 lasers," *IEEE J. Quantum Electron. (Special Issue on 1971 IEEE/OSA Conf. Laser Engineering and Applications)*, vol. QE-8, pp. 173–179, Feb. 1972.

[4] F. S. Chen, "Modulators for optical communications," *Proc. IEEE (Special Issue on Optical Communication)*, vol. 58, pp. 1440–1457, Oct. 1970.

[5] J. Dimmock, Lincoln Laboratory, private communication.

Faraday Optical Isolator/Gyrator Design in Planar Dielectric Waveguide Form

JOHN WARNER

Invited Paper

***Abstract*—The possibilities of using the magnetic Faraday effect to provide a planar dielectric waveguide isolator or circulator are studied. At least two active elements which couple the TE and TM waveguide modes are required. One of these is magnetooptic. Preliminary design data for a dielectric waveguide isolator in which the mode-converting media forms the substrate and top layer of a single waveguide structure are reported. This design should prove more practical than the optical tandem structures proposed previously.**

I. Introduction

ESSENTIAL to the proper development of integrated optical systems is the availability of the basic components for providing sources, detectors, waveguiding, modulation, switching, etc. Switching and modulation may be achieved by using electrooptic [1], acoustooptic [2] (both bulk and surface wave), and magnetooptic [3] effects to couple the TE and TM modes of waveguide propagation[1] and provide mode conversion. For example, amplitude modulation may be achieved for a TE waveguide mode by applying an ac field to an electrooptic material that forms part of the waveguide structure. There will be induced a variable coupling to the TM mode, and the TE and TM intensities will fluctuate in a complementary way. Most mode-conversion schemes are reciprocal in the sense that the effects produced are not altered by reversing the propagation. The exception to this is the longitudinal magnetooptic or Faraday effect [4] (magnetization parallel to propagation direction). Faraday rotation devices [5] have been found particularly useful in microwave waveguiding: they provide nonreciprocal transmission characteristics that have been exploited to make isolators and circulators invaluable to microwave circuitry.

In this paper we present a study of the problems and possible solutions for the fabrication of an optical planar-waveguide mode converter. It is nonreciprocal in that in the forward direction there is complete mode conversion from TE to TM and TM to TE, but in the reverse direction a TE mode will emerge as a TE mode. The nonreciprocity arises from the Faraday effect. It is well known that a linearly polarized optical beam propagating along the magnetic-field direction in an isotropic material finds its plane of polarization rotated as it proceeds. The effect is largest in ferromagnetic materials. Linearly polarized light behaves similarly in optically active materials, but the magnetic effect is uniquely different in one important respect: the "handedness" of the rotation is oppo-

Manuscript received August 10, 1973. This work was supported in part by the Advanced Research Projects Agency under ARPA Order 2327, and is published by permission of her Britannic Majesty's Stationery Office.

The author is with the Optical Physics Branch, Naval Research Laboratory, Washington, D. C. 20375. He is on leave of absence from the Royal Radar Establishment, Malvern, Worcs, England.

[1] The eigenmodes of an isotropic planar dielectric waveguide structure are TE, with the electric vector perpendicular to the plane normal, and TM, with the magnetic vector so oriented.

site for waves propagating with and against the bias magnetic field. In an optically active crystal the handedness is unaltered by a reversal of propagation direction.

Wang *et al.* [6] have studied the use of such materials in providing mode conversion between the TE and TM modes of a thin-film optical waveguide. They mention the possibility of using nonreciprocal waveguide mode converters to accomplish the circuit functions of a circulator and isolator. We borrow their terminology and examine in greater detail the design considerations for optical thin-film isolators, indicating where possible the bulk-wave analogs of the waveguide devices. In particular we propose a sandwich structure in which an isotropic guiding film separates two mode-converting media, one magnetooptic and the other anisotropic or optically active, as a more practical alternative to the tandem structures considered by Wang *et al.* [6].

II. Reflection and Mode Conversion at Film/Substrate Boundary

The mode-converting waveguide structures will consist of an isotropic film with an anisotropic substrate and/or top layers. The basic structure with coordinate axes is shown in Fig. 1. The optical dielectric constant of the film is a scalar (n_f^2), but the substrate (and top layer) have a dielectric permittivity tensor of the general form [7]

$$[\epsilon_s] = \begin{bmatrix} \epsilon_{11} & \epsilon_{12} & \epsilon_{13}^* \\ \epsilon_{12}^* & \epsilon_{22} & \epsilon_{23} \\ \epsilon_{13} & \epsilon_{23}^* & \epsilon_{33} \end{bmatrix} \tag{1}$$

We assume lossless media; $[\epsilon_s]$ is therefore Hermitian with real diagonal elements. The off-diagonal elements provide coupling between x, y, and z components of the electric field in the substrate and give rise to mode conversion. Not all of the off-diagonal elements of $[\epsilon^s]$ are nonzero. For an anisotropic crystal the off-diagonal $\epsilon_{ij}{}^s$ are real and can all be made zero by orienting the principal vibration directions [8] along x, y, and z. A subsequent rotation about x, for example, will make only ϵ_{23} and the diagonal elements ϵ_{11}, ϵ_{22}, and ϵ_{33} nonzero. Lossless gyrotropic crystals (i.e., those exhibiting magnetooptic and optically active properties) have imaginary off-diagonal $\epsilon_{ij}{}^s$ [4]. The normal situation here is that $\epsilon_{12}{}^s$ is the only nonzero off-diagonal element.

Wang *et al.* [6] have calculated the coupling matrix relating the reflected TE and TM complex field amplitudes to those of the incident waves (see Fig. 1). The coupling equation is

$$\begin{bmatrix} E_2{}^{\mathrm{TE}} \\ E_2{}^{\mathrm{TM}} \end{bmatrix} = \begin{bmatrix} r_{EE} & r_{EM} \\ r_{ME} & r_{MM} \end{bmatrix} \begin{bmatrix} E_1{}^{\mathrm{TE}} \\ E_1{}^{\mathrm{TM}} \end{bmatrix} \tag{2}$$

where

$$r_{EE} = \frac{1}{F}\left(\frac{G_1 J_2{}^*}{L_1} - \frac{G_2 J_1{}^*}{L_2}\right) \tag{3a}$$

$$r_{MM} = \frac{1}{F}\left(\frac{G_1{}^* J_2}{L_1} \frac{G_2{}^* J_1}{L_2}\right) \tag{3b}$$

$$(r_{EM})_L = \frac{2i(p_1 - p_2)n_f \cos\theta}{F\beta\epsilon_{12}} \tag{3c}$$

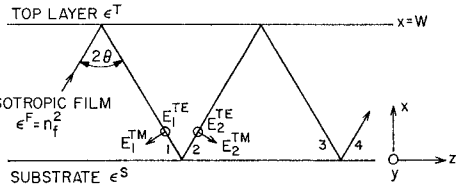

Fig. 1. The light-guiding structure, showing the E-field components and the angle of incidence (after Wang *et al.* [6]).

$$(r_{ME})_L = \frac{2i(p_1 - p_2)n_f \cos\theta}{F\beta\epsilon_{12}{}^*} \tag{3d}$$

$$(r_{EM})_P = \frac{-2(p_1 - p_2)n_f \cos\theta}{F\epsilon_{23}{}^*} \tag{3e}$$

$$(r_{ME})_P = \frac{2(p_1 - p_2)n_f \cos\theta}{F\epsilon_{23}} \tag{3f}$$

The parameters used in (3) are given below, where p_1 and p_2 are the decay constants of the evanescent waves in the substrate. The suffixes L and P refer to longitudinal ($\epsilon_{12} \neq 0$) and polar ($\epsilon_{23} \neq 0$) configurations.

$$F = (G_1 J_2/L_1) - (G_2 J_1/L_2) \tag{4a}$$

$$(G_{1,2})_L = \epsilon_{33}\cos\theta - ip_{1,2}n_f \tag{4b}$$

$$(G_{1,2})_P = p_{1,2}\epsilon_{11}\cos\theta - i(\beta^2 - \epsilon_{11})n_f \tag{4c}$$

$$J_{1,2} = n_f \cos\theta - ip_{1,2} \tag{4d}$$

$$L_{1,2} = \beta^2\epsilon_{33} - \epsilon_{11}\epsilon_{33} - \epsilon_{11}p^2{}_{1,2} \tag{4e}$$

$$(p^2{}_{1,2})_L = (1/2\epsilon_{11})\{A + \epsilon_{12}\epsilon_{12}{}^* \pm [B^2 + \epsilon_{12}\epsilon_{12}{}^*(2C + \epsilon_{12}\epsilon_{12}{}^*)]^{1/2}\} \tag{4f}$$

$$(p^2{}_{1,2})_P = (1/2\epsilon_{11})\{A \pm [B^2 - 4\epsilon_{11}\epsilon_{23}\epsilon_{23}{}^*(\beta^2 - \epsilon_{11})]^{1/2}\} \tag{4g}$$

where

$$A = \beta^2(\epsilon_{11} + \epsilon_{33}) - \epsilon_{11}(\epsilon_{22} + \epsilon_{33}) \tag{4h}$$

$$B = \beta^2(\epsilon_{11} - \epsilon_{33}) - \epsilon_{11}(\epsilon_{22} - \epsilon_{33}) \tag{4i}$$

$$C = \beta^2(\epsilon_{11} + \epsilon_{33}) - \epsilon_{11}(\epsilon_{22} - \epsilon_{33}). \tag{4j}$$

Notice that in (3a) and (3b) Fr_{EE} and Fr_{MM} are complex conjugates. We may therefore write $|r_{EE}| = |r_{MM}| = r_{11}$, giving $r_{EE} = r_{11}e^{i\phi_{EE}}$ and $r_{MM} = r_{11}e^{i\phi_{MM}}$. If we write $F = |F|e^{i\phi}$, then $\phi_{EE} + \phi_{MM} = 2\phi$.

We also assume that ϵ_{12} (or ϵ_{23}) is either real or imaginary (lossless media): Fr_{EM} and Fr_{ME} are then either real and equal but opposite ($Fr_{EM} = -Fr_{ME}$), or imaginary and equal. The scattering matrix $[r]$ in (2) will therefore take one of the following forms:

$$[r'] = \begin{bmatrix} r_{11}e^{i\phi_{EE}} & r_{12}e^{i(\phi_{EE}+\phi_{MM})/2} \\ -r_{12}e^{i(\phi_{EE}+\phi_{MM})/2} & r_{11}e^{i\phi_{MM}} \end{bmatrix} \tag{5a}$$

$$[r''] = \begin{bmatrix} r_{11}e^{i\phi_{EE}} & ir_{12}e^{i(\phi_{EE}+\phi_{MM})/2} \\ ir_{12}e^{i(\phi_{EE}+\phi_{MM})/2} & r_{11}e^{i\phi_{MM}} \end{bmatrix}. \tag{5b}$$

Equation (5) gives us the scattering matrix for a single reflection at the film/substrate boundary. A similar matrix exists for the film/top-layer boundary. For proper waveguide

modes (at the angle θ) the phase difference of the TE (and TM) waves between points 2 and 4 in Fig. 1 must be an integral multiple of 2π. This condition gives the familiar waveguide mode equations

$$\phi_{EE}{}^{S} + \phi_{EE}{}^{T} - 2Wk_0n_f \cos\theta = 2\pi m \tag{6a}$$

$$\phi_{MM}{}^{S} + \phi_{MM}{}^{T} - 2Wk_0n_f \cos\theta = 2\pi m' \tag{6b}$$

where m and m' are integers (mode orders) and $2Wk_0n_f \cos\theta$ is the phase shift experienced by a wave of free space wave number k_0 traversing from the substrate to the top layer and back. If (6a) and (6b) are not simultaneously satisfied, then the normal modes will propagate with slightly different values of θ and the mode conversion will not accumulate with successive reflections. Wang *et al.* [6] point out that for isotropic substances, $\phi_{MM} > \phi_{EE}$ and, therefore, (6a) and (6b) can only be simultaneously satisfied if at least one of the waveguide materials is optically anisotropic. We discuss the problem of achieving degenerate modes in Section V.

III. The Multiple Scattering Matrix for Degenerate Mode Coupling

The complex electric-field amplitudes of the emerging TE and TM modes after q double reflections and traverses through the film may be found by successively multiplying the mode-coupling matrices for the film/substrate and film/top-layer boundaries together with a matrix describing the phase shift $\Delta = -n_f kW \cos\theta$ introduced by a passage across the isotropic film; i.e.,

$$\begin{bmatrix} E_{2q}{}^{\mathrm{TE}} \\ E_{2q}{}^{\mathrm{TM}} \end{bmatrix} = [R] \begin{bmatrix} E_1{}^{\mathrm{TE}} \\ E_1{}^{\mathrm{TM}} \end{bmatrix}$$

where

$$[R] = \left\{ \begin{bmatrix} e^{i\Delta} & 0 \\ 0 & e^{i\Delta} \end{bmatrix} \begin{bmatrix} r_{EE}{}^{T} & r_{EM}{}^{T} \\ r_{ME}{}^{T} & r_{MM}{}^{T} \end{bmatrix} \cdot \begin{bmatrix} e^{i\Delta} & 0 \\ 0 & e^{i\Delta} \end{bmatrix} \begin{bmatrix} r_{EE}{}^{S} & r_{EM}{}^{S} \\ r_{ME}{}^{S} & r_{MM}{}^{S} \end{bmatrix} \right\}^{q}. \tag{7}$$

Wang *et al.* [6] have worked out (7) for cases where the film/top-layer boundary introduces no mode conversion ($r_{EM}{}^{T} = r_{ME}{}^{T} = 0$) and find that $[R]$ is of two types, depending upon whether the film/substrate matrix (5) corresponds to real or imaginary Fr_{EM} and Fr_{ME}. Fr_{EM} and Fr_{ME} are real if ϵ_{12} is imaginary or if ϵ_{23} is real, as would be the case for an optically active substrate, one exhibiting the Faraday effect (magnetic field parallel to propagation direction z), or an anisotropic crystal with only x corresponding to a principal vibration direction. The two multiple-scattering matrices are given by

$$[R'] = \begin{bmatrix} A & Be^{i\alpha} \\ -Be^{-i\alpha} & A \end{bmatrix}, \qquad Fr_{EM} \text{ real} \tag{8a}$$

or

$$[R''] = \begin{bmatrix} A & iBe^{i\alpha} \\ iBe^{-i\alpha} & A \end{bmatrix}, \qquad Fr_{EM} \text{ imaginary} \tag{8b}$$

where

$$A = \cos(q|r_{EM}|), \qquad B = \sin(q|r_{EM}|)$$

$$\alpha = 1/2(\phi_{EE}{}^{S} + \phi_{MM}{}^{S}) + \phi_{EE}{}^{T} + 2\Delta.$$

Complete mode conversion from TE to TM or from TM to TE will occur after q reflections if $q|r_{EM}| = \pi/2$, which is the condition for $A = 0$.

IV. Nonreciprocal Waveguide Mode Converters

An ideal nonreciprocal mode converter is one in which the mode conversion is complete in one propagation direction ($+z$) and zero in the reverse direction ($-z$). Wang *et al.* [6] have studied several configurations where mode converters and (sometimes) phase shifters are arranged in optical tandem. The scattering matrix for light passing right through the tandem structure is given by the product of the $[R]$ matrices (and phase-shift matrices if applicable), the order of multiplication depending upon the direction of propagation—forward or reverse. A change of propagation direction may alter the sign of B in the multiple scattering matrices of (8). Let us maintain a right-handed set of coordinates for both propagation directions (we choose two sets of axes so that β is positive in both cases). Since x is in the direction of the decay of the evanescent fields, it is best to choose an axis transformation equivalent to a 180° rotation about x. The Wang *et al.* [6] analysis is then formally the same for both sets of axes. If the axes in the reverse direction are x', y', and z', then

$$\begin{pmatrix} x' \\ y' \\ z' \end{pmatrix} = \begin{bmatrix} 1 & 0 & 0 \\ 0 & -1 & 0 \\ 0 & 0 & -1 \end{bmatrix} (x, y, z). \tag{9}$$

The dielectric permittivity tensors $[\epsilon_{ij}{}^{S}]$ and $[\epsilon_{ij}{}^{T}]$ have to be referred to the x'-, y'-, and z'-axes when considering propagation in the reverse direction. We find from (9) that

$$\begin{bmatrix} \epsilon_{11}' & \epsilon_{12}' & \epsilon_{12}' \\ \epsilon_{21}' & \epsilon_{22}' & \epsilon_{23}' \\ \epsilon_{31}' & \epsilon_{32}' & \epsilon_{33}' \end{bmatrix} = \begin{bmatrix} \epsilon_{11} & -\epsilon_{12} & -\epsilon_{13} \\ -\epsilon_{21} & \epsilon_{22} & \epsilon_{23} \\ -\epsilon_{31} & \epsilon_{32} & \epsilon_{33} \end{bmatrix}. \tag{10}$$

Thus we see that, in general, B will only change sign upon propagation reversal if the mode-coupling tensor element is ϵ_{12}. The exception to this is the case of optical activity where the expression for ϵ_{12} itself contains the propagation direction, and for this case a propagation direction reversal leaves ϵ_{12} unchanged.[2]

The combinations of mode converters with and without phase shifters that lead to nonreciprocal behavior are listed in Table I. Notice that they all require a magnetooptic element. The last two configurations introduce a sandwich rather than a tandem structure. Before dealing with these, however, which result from allowing the top layer to provide mode coupling, it is instructive to see how one of the tandem structures works. Take case 4 (Table I) as an example. For a polar dielectric mode converter, ϵ_{23} and Fr_{EM} are real (3e);

[2] It is this constancy of the sign of ϵ_{12} that ensures that the handedness of optical rotation is unaltered by a propagation direction reversal (see [4]).

TABLE I

LIST OF PLANAR DIELECTRIC WAVEGUIDE CONFIGURATIONS WHICH COULD EXHIBIT NONRECIPROCAL MODE CONVERSION

STRUCTURE #	ELEMENT #	LONGITUDINAL			POLAR		90° PHASE SHIFTER
		Magneto-optic ϵ_{12} imag	Optically active ϵ_{12} imag	Dielectric Anisotropy ϵ_{12} real	Magneto-optic ϵ_{23} imag	Dielectric Anisotropy ϵ_{23} real	
A - Tandem Structures							
1	1	✓					
	2						✓
	3			✓			
2	1				✓		
	2						✓
	3					✓	
3	1	✓					
	2		✓				
4	1	✓					
	2					✓	
5	1				✓		
	2			✓			
B - Layered Structures							
6	top		✓				
	bottom	✓					
7	top					✓	
	bottom	✓					

Note: The check marks (✓) indicate the element type in the structure.

from (8a) we write

$$[R_1^+] = [R_1^-] = \begin{bmatrix} A_1 & B_1 e^{i\alpha_1} \\ -B_1 e^{-i\alpha_1} & A_1 \end{bmatrix}. \tag{11}$$

The longitudinal magnetic mode converter also has a real value of Fr_{EM} because ϵ_{12} is imaginary, but ϵ_{12} and consequently B change sign upon a propagation direction reversal. Therefore,

$$[R_2^{\pm}] = \begin{bmatrix} A_2 & \pm B_2 e^{i\alpha_2} \\ \mp B_2 e^{-i\alpha_2} & A_2 \end{bmatrix}. \tag{12}$$

If we make the magnetic and dielectric mode converters complementary, i.e., $A_1 = B_1 = A_2 = B_2 = 1/\sqrt{2}$ and $\alpha_1 = \alpha_2 = \alpha$, then in the forward direction

$$[R_1^+][R_2^+] = \begin{bmatrix} 0 & e^{i\alpha} \\ -e^{-i\alpha} & 0 \end{bmatrix} \tag{13a}$$

and in the reverse direction

$$[R_2^-][R_1^-] = \begin{bmatrix} 1 & 0 \\ 0 & 1 \end{bmatrix}. \tag{13b}$$

Equation (13b) tells us that we have complete mode conversion in the forward direction yet no mode conversion in the reverse direction. The dimensions required to achieve $A = 1/\sqrt{2}$, etc., are discussed by Wang *et al.* [6].

If the top layer of the waveguide structure provides mode conversion in addition to the substrate, then the multiple scattering matrix $[R]$ given by (6) may change between the symmetric and antisymmetric forms given by (12) for forward and reverse propagation directions if one of the substrates or top layers is magnetooptic. This situation, listed in the second part of Table I, will now be considered.

We retain the assumption of an isotropic film. All of the boundaries listed in Table I for the layered structures result in the products Fr_{EM} and Fr_{ME}, (3) being real. We may therefore write $r_{EM}{}^T = -r_{ME}{}^T = r_{12}{}^T e^{i\phi_{EM}{}^T}$, and note that $|r_{EE}{}^T| = |r_{MM}{}^T| = r_{11}{}^T$ and $\phi_{EE}{}^T + \phi_{MM}{}^T = 2\phi_{EM}{}^T$, where $r_{EE} = r_{11} e^{i\phi_{EE}{}^T}$, etc. Similar expressions hold for the film/substrate coupling matrix elements. The inner part of (6) may be multiplied out to give $[R] = [R']^q$ where

$$R_{11}' = r_{11}{}^T r_{11}{}^S e^{i(2\Delta + \phi_{EE}{}^T + \phi_{EE}{}^S)} - r_{12}{}^T r_{12}{}^S e^{i(2\Delta + \phi_{EM}{}^T + \phi_{EM}{}^S)} \tag{14a}$$

$$R_{12}' = r_{11}{}^T r_{12}{}^S e^{i(2\Delta + \phi_{EE}{}^T + \phi_{EM}{}^S)} + r_{11}{}^S r_{12}{}^T e^{i(2\Delta + \phi_{MM}{}^S + \phi_{EM}{}^T)} \tag{14b}$$

$$R_{21}' = -r_{11}{}^T r_{12}{}^S e^{i(2\Delta + \phi_{MM}{}^T + \phi_{EM}{}^S)} - r_{11}{}^T r_{12}{}^T e^{i(2\Delta + \phi_{EE}{}^S + \phi_{EM}{}^T)} \tag{14c}$$

$$R_{22}' = r_{11}{}^T r_{11}{}^S e^{i(2\Delta + \phi_{MM}{}^T + \phi_{MM}{}^S)} - r_{12}{}^T r_{12}{}^S e^{i(2\Delta + \phi_{EM}{}^T + \phi_{EM}{}^S)}. \tag{14d}$$

The required solution to our problem will have real diagonal elements in $[R]$. If we assume that $r_{12}{}^T r_{12}{}^S \ll 1$, then R_{11}' and R_{22}' will be real if the TE and TM mode equations (6) are both satisfied for the chosen value of θ (and therefore Δ). Let us examine the phase angles of the off-diagonal elements of $[R']$; that for the term in $r_{11}{}^T r_{12}{}^S$ is $2\Delta + \phi_{EE}{}^T + \phi_{EM}{}^S$ in R_{12}' and $2\Delta + \phi_{MM}{}^T + \phi_{EM}{}^S$ in R_{21}'. The sum of these angles is $4\Delta + \phi_{EE}{}^T + \phi_{MM}{}^T + 2\phi_{EM}{}^S$, which is just the sum of the mode equations (5), and is therefore equal to an integral multiple of 2π. We may therefore write $e^{i(2\Delta + \phi_{EE}{}^T + \phi_{EM}{}^S)} = e^{i\alpha}$ and $e^{i(2\Delta + \phi_{MM}{}^T + \phi_{EM}{}^S)}$ as $e^{-i\alpha}$. Similar expressions hold for the terms in $r^S r^T$, and since we have assumed degenerate modes, we have the same phase angles for these terms also. $[R]$ is therefore reduced to

$$[R] = \begin{bmatrix} r_{11}{}^T r_{11}{}^S & (r_{11}{}^T r_{12}{}^S + r_{11}{}^S r_{12}{}^T) e^{i\alpha} \\ -(r_{11}{}^T r_{12}{}^S + r_{11}{}^S r_{12}{}^T) e^{-i\alpha} & r_{11}{}^T r_{11}{}^S \end{bmatrix}^q. \tag{15}$$

Sylvester's theorem [9] may be used to multiply out (15). Since we are assuming lossless media, we find from energy conservation considerations that the elements of $[R]$ are

$$R_{11} = R_{22} = \frac{\sin(q-1)\phi - A \sin q\phi}{-(B + C)} \tag{16a}$$

$$R_{12} = (B + C) \sin(q\phi) e^{i\alpha} \tag{16b}$$

$$R_{21} = (B + C) \sin(q\phi) e^{-i\alpha} \tag{16c}$$

where

$$A = r_{11}{}^T r_{11}{}^S \tag{17a}$$

$$B = r_{12}{}^T r_{11}{}^S \tag{17b}$$

$$C = r_{12}{}^S r_{11}{}^T \tag{17c}$$

$$\phi = \arctan\,[(B + C)/A]. \tag{17d}$$

Let us suppose that the substrate is magnetooptic. $r_{12}{}^S$ and, therefore, C [of (17)] will change sign upon propagation direction reversal [see text immediately following (9)]. $r_{12}{}^T$, however, does not change sign (the top layer is either polar anisotropic or optically active). It is clear from (16) that we have complete nonreciprocal mode conversion as described by (12) if $|B| = |C|$, $q\phi = \pi/2$, and $A \simeq 1$. It may be shown that $|B| = |C|$ for lossless media if $r_{12}{}^S = r_{12}{}^T$. If the top layer is an optically contacted anisotropic crystal, then $r_{12}{}^T$ is adjustable by crystal orientation. A physical picture of this type of layered structure is that in the forward direction the mode conversion at the top and bottom layers are additive and, therefore, the total mode conversion is cumulative, whereas in the reverse direction the top- and bottom-layer mode conversions mutually cancel each other and there is no net mode conversion.

V. Practical Example of a Layered Waveguide Isolator

The first concern is to devise a structure which will propagate TE and TM modes degenerately. If we assume that the TE and TM modes will have the same mode number, then (5) reduces to

$$\phi_{EE}{}^S + \phi_{EE}{}^T = \phi_{MM}{}^S + \phi_{MM}{}^T. \tag{18}$$

For small values of $\epsilon_{ij} (i \neq j)$ the phase angle ϕ_{EE} and ϕ_{MM} appearing in the waveguide mode equations (6) are given to good approximation by [6]

$$\phi_{EE} = 2 \arctan \frac{(\beta^2 - \epsilon_{22})^{1/2}}{n_f \cos\theta} \tag{19a}$$

$$\phi_{MM} = 2 \arctan \frac{(\beta^2 - \epsilon_{11})^{1/2}}{n_f \cos\theta} \frac{n_f}{\sqrt{\epsilon_{11}\epsilon_{33}}} \tag{19b}$$

where $\beta = n_f \sin\theta$ is the effective waveguide refractive index. For isotropic materials $\epsilon_{11} = \epsilon_{22} = \epsilon_{33} = \epsilon$ and $n_f{}^2 > \epsilon$; therefore $\phi_{MM} > \phi_{EE}$ and (16) is not satisfied. We must choose an anisotropic top layer in such a way that $\phi_{EE}{}^T > \phi_{MM}{}^T$ to the extent that (18) is satisfied. One solution is a positive uniaxial crystal [8, ch. 13] oriented with its optic axis in the z direction. $\epsilon_{11} = \epsilon_{22} = n_o{}^2$ and $\epsilon_{33} = n_e{}^2$. $\phi_{EE}{}^T - \phi_{MM}{}^T$ is therefore > 0 for values of n_f between n_o and $\sqrt{n_o n_e}$. This is illustrated in Fig. 2 where $(\phi_{EE}{}^T - \phi_{MM}{}^T)$ is plotted against n_f for various values of β. Also plotted on the graph is $\phi_{MM}{}^S - \phi_{EE}{}^S$ versus n_f for an isotropic substrate layer. The marked intersections are the points of degeneracy. Just which refractive index combinations produce degenerate mode propagation is best seen by plotting graphs such as Fig. 3 where curves of n_f versus β for given n_t are plotted—all for a given positively uniaxial top layer (HgS in this example). Wang *et al.* [6] show that performance characteristics that are more tolerant of waveguide dimensions, etc., result from a choice of materials giving the larger $|r_{EM}|$. Large values of $|r_{EM}|$ will be obtained by making the TE- and TM-mode evanescent waves penetrate the substrate and top layer by large and, if possible, equal amounts. We would therefore like to operate our mode converter with β close to the cutoff value (larger than n_T or n_S). If we write $\phi = \phi_{EE}{}^S + \phi_{EE}{}^T - \phi_{MM}{}^S - \phi_{MM}{}^T$ then, in general,

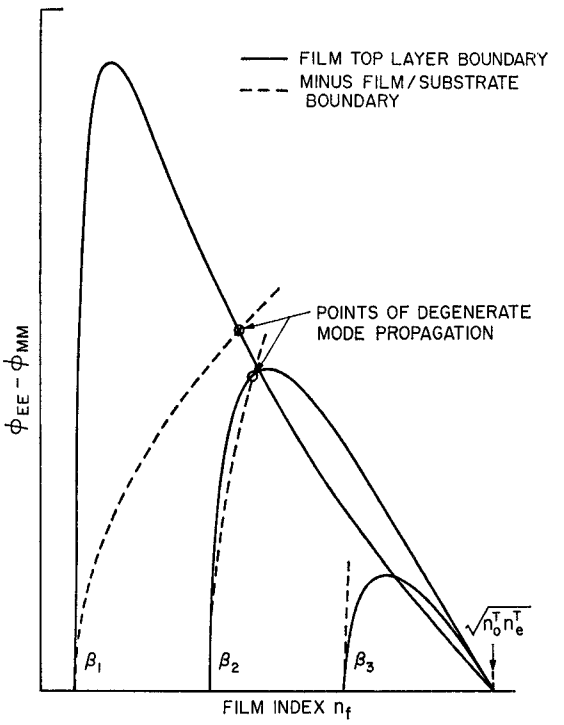

Fig. 2. Plot of $\phi^{EE^T} - \phi^{MM^T}$ (solid curves) and $\phi^{MM^S} - \phi^{EE^S}$ (dotted curves) versus film refractive index for given positive uniaxial top layer and isotropic substrate. The effective guide index β characterizes each graph and has a value equal to the smaller intercept on the n_f axis.

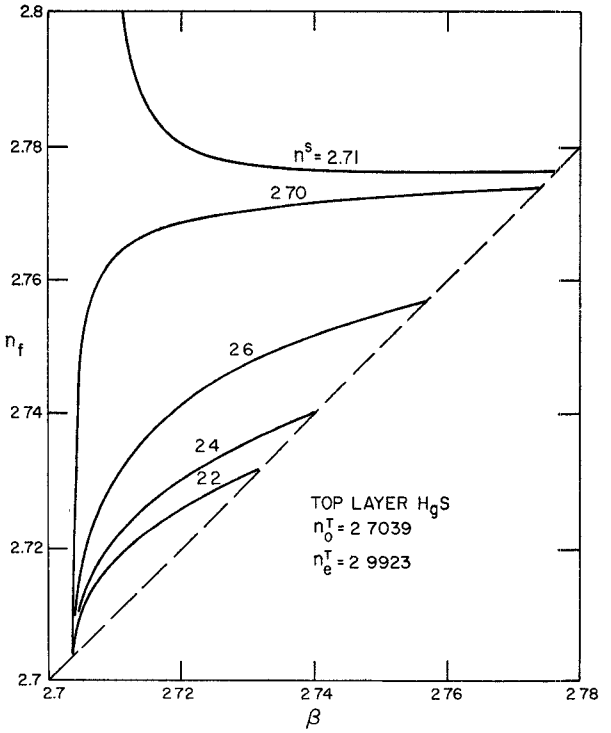

Fig. 3. Family of curves indicating the possible combinations of n_f, n_s, and β, which will give degenerate mode propagation when associated with a positive uniaxial top layer (HgS in this example, $n_o = 2.704$ and $n_e = 2.992$ at 1.152 μm).

$d\phi/d\theta$ increases as β approaches cutoff. A large value of $d\phi/d\theta$ implies that the film thickness for degenerate modes becomes critical again despite the large value of $|r_{EM}|$ obtained by operating near cutoff. This is not always the case, however; Fig. 4 shows that if the substrate refractive index is larger than a certain amount, then $d\phi/d\theta$ actually decreases as β approaches cutoff. Other factors remain, however, which get worse closer to cutoff; optical scattering from surface imperfections increases dramatically [10]. In fact, structures which use the positive birefringence scheme (which we have just outlined) to achieve degenerate mode operation will always be close to cutoff, merely because the refractive indices have to be within the range n_o^T and $\sqrt{n_o^T n_e^T}$, and optical birefringes are never very large.

An alternative way to satisfy (16) is to use a *negative* uniaxial crystal, oriented with its optic axis along (or near) the y direction. $\epsilon_{22}=n_e^2$ is now smaller than $\epsilon_{11}=n_o^2$, and $(\beta^2-\epsilon_{11})<(\beta^2-\epsilon_{22})$. n_f can now go to larger values before $\phi_{EE}{}^T-\phi_{EE}{}^M<0$, which in turn may permit degenerate mode propagation at β sufficiently far from cutoff for optimum performance.

As an example of a possible practical waveguide isolator we consider a structure formed by sputtering an isotropic film of As_2S_3 onto a YIG substrate and optically contacting an $LiNbO_3$ crystal to form the top layer. The latter is oriented with its optic axis in the plane of the film close to the y direction. The amount of offset is adjustable to provide a mechanism for adjusting $r_{12}{}^T$ to match $r_{12}{}^S$, which is itself set by the optical rotation coefficient of YIG. The design parameters are summarized in Table II.

The major weakness of this design is the close tolerance placed on the film thickness. This is due mainly to the weakness of the magnetooptic coupling in the substrate. Since the coupling per reflection is so weak, many reflections are required to achieve complete mode conversion. Mode degeneracy has to be maintained over greater distances and, therefore, the film thickness should be kept very constant. Unfortunately, the Faraday effect cannot be made much larger than that for YIG at 1.152 μm without also increasing absorption losses to an intolerable degree. The magnetooptic layer is essential to the nonreciprocal nature of the device. A possible solution to the dilemma of providing stronger magnetooptic mode coupling would be to make the waveguide film magnetooptic rather than the substrate. Except for very weakly guiding structures (small differences in refractive indices), most of the electromagnetic field is in the film and not in the substrate. We are currently studying this problem.

The anisotropic top-layer coupling is, however, very strong. Notice that an orientation offset of only one-half degree should be sufficient to match the magnetooptic mode conversion. A convenient way to provide an experimentally adjustable coupling would be to rotate the top-layer crystal well beyond the required amount and to press the crystal onto the film/substrate assembly with an adjustable force in the same manner as for prism couplers; a variable air gap will produce a variable amount of mode coupling.

VI. Summary

We have used and extended the analysis of Wang *et al.* [6] for mode-converting optical waveguide structures to study the problems of designing a nonreciprocal mode converter. A magnetooptical material is required, but at least one other complementary element is also needed. We propose a layered structure in which the magnetic and anisotropic materials are separated by an isotropic film. Reorientation of the anisotropic film permits experimental control of matching the mode-conversion coefficients, and we suggest that such a

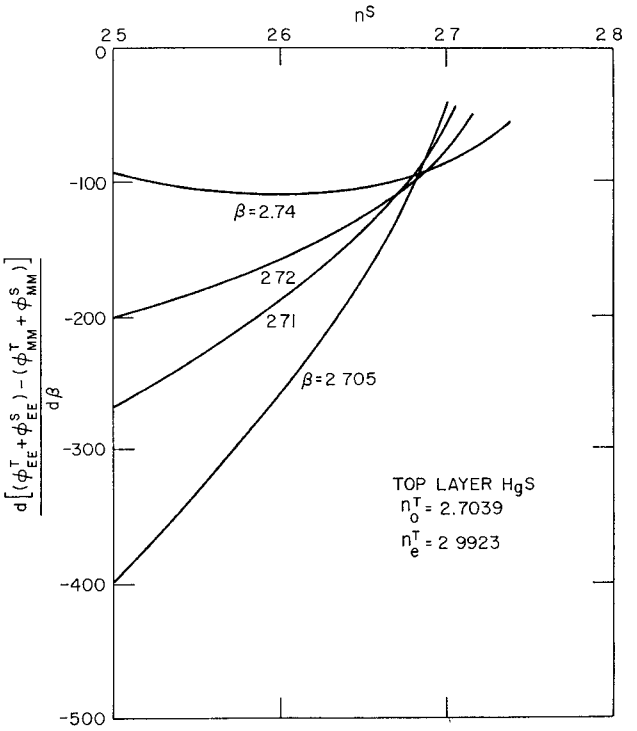

Fig. 4. Graphs of $d(\phi^{EES}+\phi^{EET}\times\phi^{MMS}\times\phi^{MMT})/d\beta$ versus n_s (assumed isotropic) plotted for degenerate mode propagation with various values of β (HgS top layer, $n_o=2.704$ and $n_e=2.992$ at 1.152 μm).

TABLE II

Numerical Data Summary for a Proposed Layered-Structure Faraday Isolator/Gyrator Using $Y_3Fe^5O_{12}$, Ag_2S_3, and $LiNbO_3$ Operating at 1.152 μm

LAYER	MATERIAL	REFRACTIVE INDICES	PERMITTIVITY	COMMENTS
Top	$LiNbO_3$ Ref. [11]	$n_o = 2.228$ $n_e = 2.151$	$\epsilon_{11} = \epsilon_{33} = 4.963$ $\epsilon_{22} = 4.627$ $\epsilon_{23} = -.002$	Optic axis set about 0.4 degrees from y in yz plane to achieve $\lvert r_{EM}^T\rvert = \lvert r_{EM}^S\rvert$
Film	As_2S_3 Ref. [12]	$n_f = 2.46$		Film thickness to be 0.90 $\pm$ .002 for first order mode degenerate
Substrate	$Y_3Fe_5O_{12}$ Ref. [13]	$n_s = 2.228$	$\epsilon_{11} = \epsilon_{22} = \epsilon_{33} = 4.963$ $\epsilon_{12} = i3{\cdot}4\times10^{-4}$	Magnetized along propagation direction z. Faraday rotation given in Ref. [13] as 280°/cm

Waveguide effective refractive index $\beta = 2.292$ ($\theta = 69.1$ deg).
Critical angle at film/substrate boundary $\theta_c = 64.9$ deg.
$|r_{EM}^T| = |r_{EM}^S| = 0.00055$
Estimated interaction pathlength = 6.6 cm.[3]

[3] This estimate is based on multiplying the distance down the guide per double reflection by the number of reflections required to give complete mode conversion. In some cases the Goos–Haenchen shift will cause this distance to be somewhat larger. (See H. Kogelnik, T. P. Sosnowski, and H. P. Weber, paper presented at the Spring 1973 Meeting Opt. Soc. Amer., TUG 18; also in *IEEE J. Quantum Electron.*, vol. QE-9, pp. 795–800, Aug. 1973.)

structure lends itself more readily to practical implementation than do the tandem structures proposed by Wang *et al.* [6]. Preliminary design data are presented for a YIG–As_2S_3–$LiNbO_3$ structure. Finally, we note that it might be more practical to provide a magnetic film rather than a magnetic substrate [3]. Studies of such a layered structure are underway, and we believe that this, too, could lead to a useful nonreciprocal isolator device.

ACKNOWLEDGMENT

The author wishes to thank W. K. Burns, T. G. Giallorenzi, and A. F. Milton for many stimulating discussions.

REFERENCES

[1] a) W. S. C. Chang and K. W. Loh, "Theoretical design of guided wave structure for electrooptical modulation at 10.6 μm," *IEEE J. Quantum Electron.*, vol. QE-8, pp. 463–470, June 1972.
b) D. Hall, A. Yariv, and E. Garmire, *Opt. Commun.*, vol. 1, p. 403, 1970.
c) D. Russo and J. Harris, *Appl. Opt.*, vol. 10, p. 2768, 1971.
[2] a) W. S. Chang, "Acoustooptical deflections in thin films," *IEEE J. Quantum Electron.*, vol. QE-7, pp. 167–170, Apr. 1971.
b) L. Kuhn, P. F. Heidrich, and E. G. Lean, *Appl. Phys. Lett.*, vol. 19, p. 428, 1971.
[3] P. K. Tien, R. J. Martin, R. Wolfe, R. C. LeCraw, and S. L. Blank, *Appl. Phys. Lett.*, vol. 21, pp. 394–396, Oct. 1972.
[4] L. D. Landau and E. M. Lifshitz, *Electrodynamics of Continuous Media.* Elmsford, N. Y.: Pergamon, 1960, pp. 331 *et seq.*
[5] J. Helszajn, *Principles of Microwave Ferrite Engineering.* New York: Wiley, 1969.
[6] S. Wang, M. Shah, and J. D. Crow, *J. Appl. Phys.*, vol. 43, no. 4, p. 1861, 1972.
[7] P. S. Pershan, *J. Appl. Phys.*, vol. 38, p. 1482, 1967.
[8] J. F. Nye, *Physical Properties of Crystals: Their Representation by Tensors and Matrices.* London, England: Oxford, 1957.
[9] R. A. Frazer, W. J. Duncan, and A. R. Collar, *Elementary Matrices.* Cambridge, England: Cambridge, 1952, p. 78.
[10] P. K. Tien, *Appl. Opt.*, vol. 10, p. 2395, Nov. 1971.
[11] M. V. Hobden and J. Warner, *Phys. Lett.*, vol. 22, pp. 243–244, 1966.
[12] L. Bornstein, *Physcial Tables*, vol. 2, part 8. Berlin, Germany: Springer, 1962, pp. 2–427.
[13] ——, *Tables* (New Series), group III, vol. 4a. Berlin, Germany: Springer, 1970, p. 344.

Periodic Structures and Their Application in Integrated Optics

WILLIAM S. C. CHANG, SENIOR MEMBER, IEEE

Invited Paper

***Abstract*—Periodic structures are used widely in integrated optics for input–output couplers, bandstop filters, modulators, directional couplers, and distributed feedback lasers. An analytical discussion and review of these devices is given based upon the coupled-mode transmission-line analysis. Experimental results and performance characteristics are presented to illustrate the special features of each type of device. Finally, the usefulness of transmission-line analysis to the understanding and the design of these devices is pointed out.**

I. INTRODUCTION

INTEGRATED optics is an ambitious attempt to apply thin-film and integrated electronics technology to optical circuits and devices [1]–[8]. One of its goals is to achieve sophisticated thin-film and fiber optical communication and data processing systems. We may envision that such systems will eventually be comparable to present microwave systems, complete with thin-film sources, detectors, waveguides, filters, directional couplers, modulators, etc. [7], [8]. Naturally, there is a great deal of similarity between microwave and integrated optical components. However, because of the shorter optical wavelength, many microwave techniques utilizing the matching of the transverse field variations for the fabrication of devices such as E–H tuners, magic T's, etc., are not applicable. Instead, techniques using periodic structures play a dominant role in integrated optical device fabrication. There are two major advantages in the use of periodic structures: a) although the individual interactions from each element in the periodic structure are small, their phase synchronized cumulative effects can be very large; and b) small amounts of random defects created in the fabrication process will not affect the characteristics of the device significantly. Applications of periodic structures in integrated optics have already led to the achievement of a number of devices such as the input–output grating coupler [9]–[12], the bandstop filter [13], distributed feedback lasers [14]–[16], modulators [17]–[22], and directional couplers [23].

Despite the fact that both the properties and the fabrication techniques of different devices using periodic structures vary a great deal, there is a considerable amount of similarity in their analyses. It is informative to review the properties of the various applications of periodic structures in integrated optics, one by one, from a unified coupled-mode transmission-line analysis point of view. Design data, experimentally measured properties, and performance characteristics will then be discussed to point out the special features of each

Manuscript received August 1, 1973. This work was supported in part by the NSF under Grant GK31854 to Washington University.

The author is with the Department of Electrical Engineering and the Laboratory for Applied Electronic Sciences, Washington University, St. Louis, Mo. 63130.